Redox analysis of the cytochrome *o*-type quinol oxidase complex of *Escherichia coli* reveals three redox components

Barbara BOLGIANO,*‡§ Ian SALMON,† W. John INGLEDEW‡ and Robert K. POOLE*‖

* Microbial Physiology Research Group, Kings College London, Campden Hill Road, London W8 7AH, U.K., † Biological Laboratory, University of Kent, Canterbury, Kent CT2 7NJ, U.K., and ‡ Department of Biochemistry and Microbiology, University of St. Andrews, St. Andrews, Fife KY16 9AL, Scotland, U.K.

Potentiometric analyses of the cytochrome *o*-type oxidase of *Escherichia coli*, using membranes from a strain containing amplified levels of the cytochrome *bo* complex, were conducted to resolve the redox centres of the oxidase. The cytochrome *o*-type oxidase of *E. coli*, a quinol oxidase, contains 2 mol of *b*-type haem per mol of complex and copper. Detailed analysis of potentiometric titrations, based on the absorbance of the Soret band, suggests that there are three contributions with midpoint potentials ($E_{m,7}$) around +55 mV, +211 mV and +408 mV, all with maxima at 426–430 nm in the reduced state. In the α region of the spectra, a component with $E_{m,6.85} = +58$ mV has a maximal peak at 557 nm, and twin peaks at 556 and 564 nm titrate with $E_{m,6.85} = +227$ mV. A feature corresponding to the highest potential Soret contribution was not observed. These data can be explained either by a model incorporating haem–haem interaction or by attributing the shorter-wavelength band (557 nm) to haem *b* and a split α-band (556, 564 nm) to the haem *o* (oxygen-binding haem *b*). Absolute spectra of oxidized membranes show continuous absorbance from 460 to 530 nm and suggest the presence of a high-spin haem component in the membranes. Monitoring absorbance at 635 minus 672 nm, contributions with midpoints ($E_{m,7}$) around +52 mV, +234 mV and +371 mV are observed. This latter contribution is possibly the highest-potential component which titrates with $E_m > +400$ mV in the Soret region and may represent copper–haem coupling in the cytochrome *o* complex.

INTRODUCTION

The spectroscopic methods of Chance, Smith and Castor, developed over 35 years ago, identified cytochrome *o* in many bacteria, including *Escherichia coli* (Chance *et al.*, 1953; Castor & Chance, 1959). More recent investigations have revealed that these cytochrome *o*-type oxidases differ from each other in a number of properties, such as redox behaviour, CO complexation (reviewed by Poole, 1988) and immunological cross-reactivity (Kranz & Gennis, 1985).

The cytochrome *o*-type oxidase of *E. coli* is the predominant oxidase in well-aerated exponentially growing cultures; the alternative cytochrome *d*-type oxidase is expressed in anaerobic culture or under conditions of low aeration, as in the stationary phase of growth (Georgiou *et al.*, 1988; reviewed by Poole & Ingledew, 1987).

A significant degree of similarity has been found between the predicted amino acid sequence of the larger subunits of the *E. coli* cytochrome *bo* complex and the sequences of the corresponding subunits of cytochrome aa_3-type oxidases (Chepuri *et al.*, 1990). Subunit I of the latter contains many conserved residues, and is thought to bind both haems and at least one copper atom in both the *Paracoccus* and bovine heart cytochrome oxidases (Müller *et al.*, 1988; Holm *et al.*, 1987). Less extensive sequence similarity has also been found between other subunits in the *E. coli* oxidase and those of the aa_3 complexes. As with the aa_3-type oxidase (Wikström *et al.*, 1981), the cytochrome *bo* complex contains both high-spin ($g = 6.0$) and low-spin ($g = 3.0$) haems (Hata *et al.*, 1985), and evidence of haem–haem and haem–copper co-operativity, similar to that seen in cytochrome aa_3 (Wilson & Leigh, 1972) has recently been demonstrated in the *E. coli* cytochrome *bo* complex (Salerno *et al.*, 1989, 1990). The cytochrome *o*-type oxidase of *E. coli* has also been found by low-temperature ligand-exchange methodology to form an oxygen-binding complex (Poole & Chance, 1981; Poole *et al.*, 1979) resembling compound A of cytochrome a_3 (Erecinska & Chance, 1972; Chance *et al.*, 1978). Taken together, the evidence suggests that an oxygen-reactive binuclear centre exists in the *E. coli* cytochrome *o*-type oxidase (*o*–Cu) that is analogous to the bovine heart a_3–Cu_B redox centre (Salerno *et al.*, 1989, 1990).

A controversy exists, however, over the midpoint oxidation–reduction potential(s) of the components of the *bo* complex. On the basis of optical spectroscopy at room temperature, Kita *et al.* (1984) showed that the purified four-subunit (Matsushita *et al.*, 1984) cytochrome *bo* complex has a single $E_{m,7.4} = +125$ mV with a pH-dependence of −60 mV/pH. In membranes from a strain lacking the cytochrome *d*-type oxidase, midpoint oxidation–reduction potentials at pH 7.0 of +20 mV (presumed to be from the succinate dehydrogenase cytochrome b_{556}; Kita *et al.*, 1989) and +165–170 mV (Lorence *et al.*, 1984) have been found. The higher-potential component was assigned to the cytochrome *o*, since, in the presence of CO, only components of $E_{m,7} = +21$ and +310 mV were observed (Lorence *et al.*, 1984). Recently, from e.p.r. spectra at 15 K, for an *E. coli* strain that produces an amplified level of the cytochrome *o* complex, but which lacks the *d*-type oxidase, both high- and low-potential midpoint values at pH 7.0, around +180 mV and +280 mV, were identified for both the high- and low-spin haems. A third redox transition at $E_{m,7}$ around +370 mV were observed and assigned to the Cu(I)/Cu(II) transition (Salerno *et al.*, 1990). Here we present our findings from optical spectra, using the same strain in room-temperature redox titrations.

§ Present address: M.R.C. Clinical Research Centre, Watford Road, Harrow, Middx. HA1 3UJ, U.K.
‖ To whom all correspondence should be addressed.

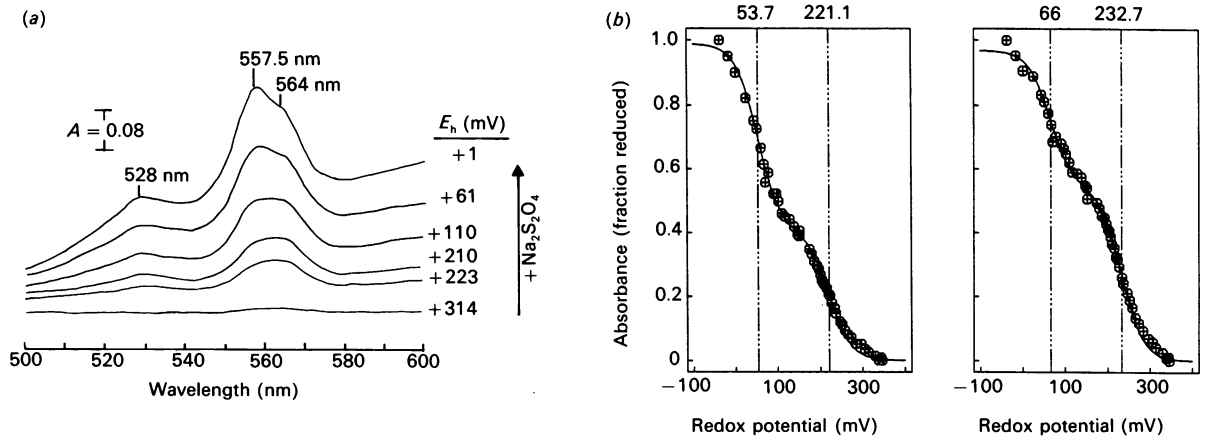

Fig. 1. Potentiometric titration of *E. coli* RG145 membranes by difference spectroscopy (500 to 600 nm) at 25 °C

(*a*) Difference spectra from 500–600 nm recorded during a reductive titration using 575 nm as reference wavelength, displaced vertically for clarity. The samples shown were poised at +314, +223, +210, +110, +61 and +1 mV by using a ferricyanide-oxidized (+344 mV) sample as the subtracted baseline. Sodium dithionite was used as reductant. Scan rate, 1.4 nm/s. (*b*) Best-fit analysis from measurements at 557.5 minus 580 nm (left) and 564 minus 580 nm (right). The solid lines represent the best-fit analyses (sum of squares = 0.01 and 0.07 respectively) for two components with midpoint potentials ($E_{m,6.85}$) of +54 and +221 mV at 557.5 nm and +68 and +232 mV at 564 nm. Membranes were suspended in 100 mM-Tes/4 mM-EDTA, pH 6.85, at a concentration of 8.6 mg/ml.

MATERIALS AND METHODS

Strains and growth conditions

E. coli strains RG145 and GO103 were kindly provided by Dr. R. B. Gennis, University of Urbana, IL, U.S.A. Strain RG145, a cytochrome *o* oxidase over-expressing strain, which lacks cytochrome *d* (Au & Gennis, 1987), was grown at 37 °C at high aeration on '56' media (Gibson *et al.*, 1977), pH 7.0, supplemented with a Mo- and NO_3^--free trace-elements solution (Pirt, 1967; 10 ml/l), Luria broth (Miller, 1972; 50 ml/l) and glycerol (4 ml/l). After being autoclaved, the medium was aseptically supplemented with nicotinic acid and thiamin hydrochloride (each at 0.5 mg/l final concn.), $MgCl_2$ (1 mM final concn.) and ampicillin (100 μg/ml final concn.). A 500 ml 18.5 h starter culture grown in a 2-litre flask to an apparent A_{600} of 3 (corrected for dilution) was used as inoculum for a 10-litre batch growth in a stirred Biostat V fermenter (Braun) sparged with air at 8 l/min. Cells were harvested in the stationary phase of growth (apparent A_{600} of 3 after correction for appropriate dilution) at 17–24 h by centrifugation in an Alpha-Laval continuous-flow centrifuge and subsequently by centrifugation of the slurry at 12500 *g* for 15 min, and were then kept frozen at −20 °C. Cells typically contained 0.32 nmol of cytochrome *o*/mg of protein, a 6-fold amplification over wild-type cells, e.g. AN2342 (Poole *et al.*, 1989), which contained 0.053 nmol of cytochrome *o*/mg of protein.

Strain GO103 (deficient in cytochrome *d*) was grown in a glycerol minimal medium as described in Salerno *et al.* (1989) supplemented with the trace elements (final concns. as follows): $FeCl_3,6H_2O$ (1.77 μM); $CaCl_2,6H_2O$ (2.45 μM); $ZnCl_2$ (14.7 μM); H_3BO_3 (4.7 μM); and $CoSO_4,7H_2O$ (0.68 μM). Membranes of strain GO103 were prepared as described by Rothery *et al.* (1987).

Cytoplasmic membrane preparation from strain RG145

All procedures were carried out at 4 °C. Thawed cells were washed twice with a buffer containing 0.1 M-Tes, 20 mM-magnesium acetate, 0.25 M-sucrose and 0.25 mM-EGTA (pH 7.0) and were resuspended to approximately one-tenth the original volume in the same buffer. To a homogenized suspension was added the proteinase inhibitor phenylmethanesulphonyl fluoride (1 mM final concn.) and a few grains of proteinase-free DNAase I. Cells were broken by passing the suspension through a French pressure cell (Aminco) (138 MPa); the cell lysate was the supernatant fraction obtained by centrifugation at 12500 *g* for 20 min. Membrane fragments were then obtained by centrifuging the lysate at 150000 *g* for 90 min at 4 °C. The membrane fraction was suspended in 50 mM-Tes/5 mM-EDTA, pH 7.0, homogenized and re-spun as above. The washed membranes were resuspended in the Tes/EDTA buffer, homogenized and frozen. Membranes contained around 0.52 nmol of cytochrome *o*/mg of membrane protein.

Potentiometric titrations

Redox titrations were based on the method of Dutton (1978). Oxidation–reduction potentials were measured with a Beckman model 4500 digital pH/mV meter using a combination platinum and calomel electrode (Russell pH Ltd., Auchtermuchty, Fife, Scotland, U.K.). The meter was calibrated by immersing the electrode in a solution (E_h = +429 mV) containing 10 mM-$K_4Fe(CN)_6$, 10 mM-$K_3Fe(CN)_6$ and 150 mM-Tes/3 mM-EDTA, pH 7, bubbled with argon. Tirations were carried out at 25 °C in an anaerobic glass cuvette of approx. 1 cm path-length and 10 ml working volume. The sample consisted of a membrane suspension (about 10 mg of protein/ml) in 150 mM-Tes/2 mM-EDTA, pH 7.0, and the following redox mediators ($E_{m,7.0}$ in mV, concentration in μM): quinhydrone (+280, 50); 2,3,5,6-tetramethylphenylenediamine (+260, 20); 1,2-naphthoquinone-4-sulphonate (+215, 20); 1,2-naphthoquinone (+143, 20); *N*-methylphenazonium methosulphate (+80, 20); menadione (+9, 20); 2-hydroxy-1,4-naphthoquinone (−145, 20), benzyl viologen (−311, 2). The cuvette and sample were flushed with moistened argon for 45 min before and during the titration. The sample was stirred by a 12 mm-long magnetic stir bar driven from the outside of the cuvette with a Citenco Microstir (Park Products, Blackburn, Lancs., U.K.), to the shaft of which was attached a button magnet (Gallenkamp). Sodium dithionite was used as reductant and sodium ferricyanide or ammonium persulphate were used as oxidants. Oxidant and reductant solutions were prepared in 150 mM-Tes/2 mM-EDTA, pH 7.0, which had been bubbled with argon. These solutions were kept in stoppered tubes on ice throughout the experiment. The use of ammonium

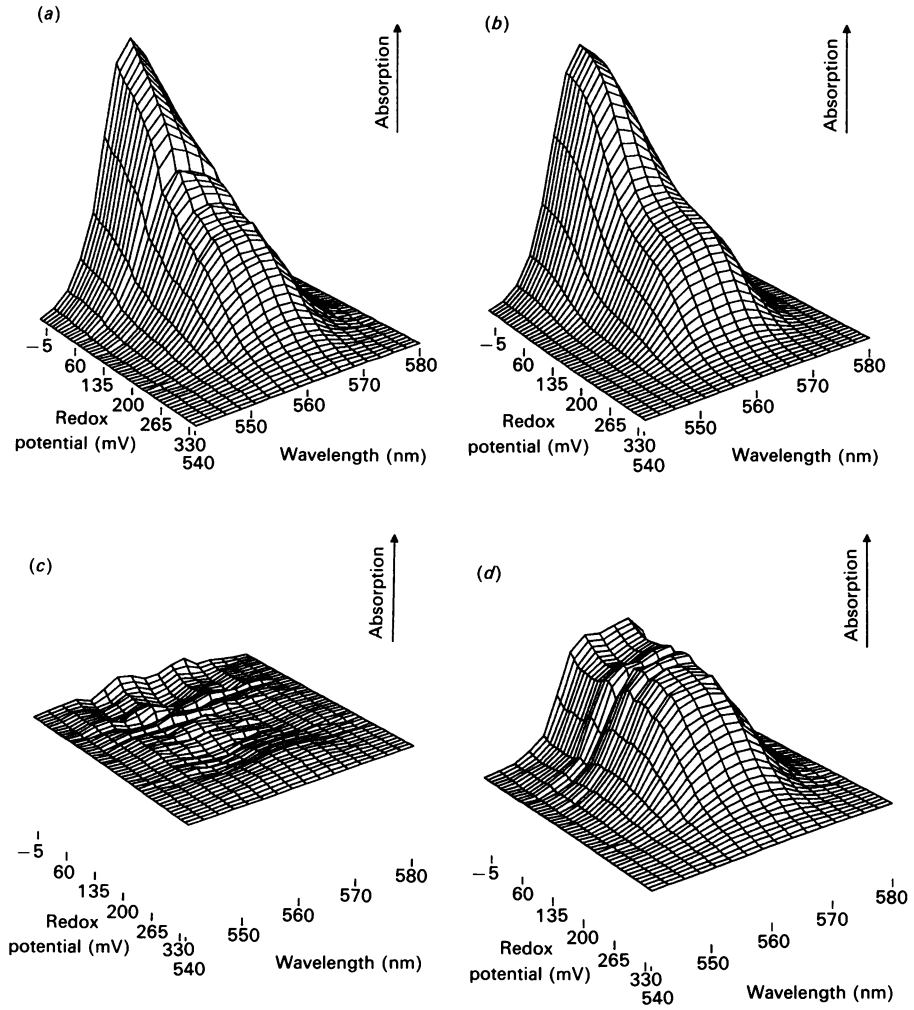

Fig. 2. Predicted redox surface for a two-redox component three-spectral component fit (540 to 580 nm)

(*a*) Original data plotted on a regular grid (10 mV and 2.5 nm steps). (*b*) Predicted surface based on two redox components, three spectral components. (*c*) Difference (scaled 2.5 ×) between the actual and predicted data shown in graphs (*a*) and (*b*). (*d*) Original data minus a component titrating with a midpoint at +58 mV.

persulphate permitted the monitoring of absorption in the Soret (400–450 nm) region. Additions were made with a 25 μl Hamilton syringe fitted with a 70 mm-long needle, and the titrations were performed in both the oxidative and reductive directions. Spectra were taken at every 15–25 mV change with the stirrer off to prevent noise. The pH was maintained to within 0.1 pH unit over the course of the titration.

Spectrophotometry

Difference spectra were recorded with a Johnson Foundation DBS-3 dual-wavelength scanning spectrophotometer as described by Williams & Poole (1987). A 1 mm slit (4 nm spectral bandwidth) was used and the cuvettes had an optical path-length of 1 cm. The reference wavelength was set at 575 nm, or, when scanning the Soret region exclusively, at 455 nm. During a redox titration, a fully reduced or fully oxidized scan was usually used as a reference. To obtain absolute spectra, a 6% (w/v) suspension of low-fat dehydrated milk dissolved in buffer was prepared as a turbid reference, and the difference in absorbance between the sample and milk was taken as the absolute spectrum.

Analysis of oxidation–reduction titration data

The redox potential of a system is related to the ratio of oxidized to reduced species of a component capable of taking part in redox reactions, by the Nernst equation. Redox analyses are generally presented as a plot of the total amount of the reduced species (as indicated by the absorption due to cytochrome reduction) versus the redox potential of the medium. If, however, components have similar E_m values or are present at greatly different concentrations, the component curves are not resolvable by eye, and computer modelling may be applied.

At any point in the titration the degree of overall reduction in the spectrum is given by:

$$X = \sum_{i=1}^{m} \frac{A_i}{1 + e^{(E_h - E_{m,i})/c}}$$

where A_i represents units of complete reduction for component i and $c = \boldsymbol{RT}/nF$, E_h is the redox potential of the medium relative to the hydrogen electrode, E_m is the midpoint potential, $\boldsymbol{R}$ is the universal gas constant, F is Faraday's constant, T is the absolute temperature and n is the number of electrons transferred from reduced to oxidized forms.

The sum of the differences squared between experimental values and those predicted by the above function was minimized by using a quasi-Newton algorithm (Gill & Murray, 1972) as

implemented in routine E04KBF of the NAG (mark 13) FORTRAN library. The calculations were performed on an HLH Clipper computer.

Analytical methods

Protein concentrations were determined by the method of Markwell *et al.* (1978), with BSA as a standard. The following absorption coefficients for the calculation of cytochromes *b* and *o* at room temperature were taken from Kita *et al.* (1984): $\epsilon_{415-430} = 145\ mM^{-1} \cdot cm^{-1}$ for cytochrome *o* from CO difference (CO + reduced minus reduced) spectra and $\epsilon_{560-580} = 18.7\ mM^{-1} \cdot cm^{-1}$ for cytochrome *b* from fully reduced minus fully oxidized spectra. Pyridine haemochrome spectra were measured in 2.1 M-pyridine/0.2 M-NaOH by the Falk method (Fuhrhop & Smith, 1975). Acid/acetone extraction of haems was performed as described by Rieske (1967).

Chemicals

General reagents were from Fisons or BDH Chemicals and were of AnalaR grade wherever possible. 1,2-Naphthoquinone was from ICN Pharmaceuticals (Plainview, NY, U.S.A.), 1,2-naphthoquinone-4-sulphonic acid was from Koch–Light Laboratories and 2,3,5,6-tetramethylphenylenediamine was from Aldrich Chemical Co. BSA, Tes, phenylmethanesulphonyl fluoride, proteinase-free DNAase I, 2-hydroxy-1,4-naphthoquinone, benzyl viologen and phenazine methosulphate were from Sigma Chemical Co. Ar, O_2-free N_2 and CO were from BOC Special Gases.

RESULTS

Room-temperature redox titrations (540 to 580 nm)

To characterize the cytochrome *bo* complex of strain RG145 of *E. coli*, which over-expresses cytochrome *o* but lacks the cytochrome *d* complex (Au & Gennis, 1987), potentiometric analyses were performed at 25 °C, monitoring redox changes optically. Contributions at about 557.5 nm and 564 nm could be distinguished throughout the titration in difference spectra with the oxidized sample as baseline (Fig. 1*a*). Both of these peaks are attributed largely to the oxidase, being observed in reduced-minus-oxidized difference spectra of the purified enzyme at 77 K (Kita *et al.*, 1984). The redox titration can be analysed (Fig. 1*b*) in terms of two components absorbing maximally at 557.5 nm and 564 nm each having E_m values of 54–68 mV and 221–232 mV. At 557.5 nm the relative contribution of each is 58 % and 41 %, whereas at 564 nm the relative contribution of each is 37 % and 55 %. Somewhat higher E_m values (195–199 mV) and 291–292 mV) were observed at 77 K (result not shown). In some titrations there was a small contribution from a lower-potential component.

When membranes from strain GO103 of *E. coli*, which also lacks the cytochrome *d* oxidase but which synthesizes cytochrome *o* from chromosomal genes only, were subjected to a similar titration, two components with $E_{m,7.0}$ of +86 mV (52 %) and +231 mV (45 %) were observed when the absorbance change of the broad peak at 560 nm was monitored (results not shown).

A more detailed analysis of strain RG145 was performed by fitting the data from a redox surface (that is, at every 2.5 nm from 540 nm to 580 nm) in addition to using the area under the curves. From analyses across the surface in the wavelength and redox directions, the relative intensities, bandwidths and ab-

Table 1. Area and surface analyses of potentiometric titrations of RG145 membranes (540–580 nm)

Shown are the best-fitting parameters for two- and three-component fits determined from analysis of the area under absorbance peaks (column 1), analysis of each wavelength interval in the redox surface (column 2) and the best-fitting wavelengths, spectral contributions and bandwidths (assuming a Gaussian function) with fixed midpoints (column 3). Sum-of-square values of statistical fit are included.

Column 1 (area)		Column 2 (surface)				Column 3 (fixed midpoints)			
$E_{m,6.85}$ (mV)	Amount	$E_{m,6.85}$ (mV)	Amount	$\lambda_{max.}$ (nm)	Bandwidth (nm)	$E_{m,6.85}$	Amount	$\lambda_{max.}$ (nm)	Bandwidth (nm)
Two-component fits									
57	0.52	57	0.59	556.9	13.4	58	0.58	557.1	14.0
226	0.44	227	0.45	561.4	16.1	227	0.28	556.0	9.3
						227	0.38	564.8	11.2
Sum of squares = 0.013			Sum of squares = 0.281				Sum of squares = 0.129		
Three-component fits									
52	0.51	55	0.56	557.3	14.4				
207	0.34	215	0.30	555.8	9.0				
273	0.12	233	0.38	564.8	11.4				
Sum of squares = 0.007			Sum of squares = 0.079						

sorption maxima of the redox components may be obtained. Results of two-component fits to redox data based on the area under titration curves (Fig. 2*a*) show midpoints ($E_{m,7}$) of +57 mV (52%) and +226 mV (44%), while the three-component fit to the same data gave E_m values of +52 mV (51%), +207 mV (34%) and +273 mV (12%) (Table 1, column 1, and Fig. 2*b*). Analysing the redox data at each wavelength shows that the +55 mV component has a wavelength maximum around 557 nm and that the +210–220 mV component appears as a broad or split peak with absorption maxima at 558 and 562 nm. With the data cast on a regular mesh, analysis of the redox surface gives a two-component fit with good correlation between midpoints obtained from this analysis and those predicted from the curve areas (Table 1, column 2 and Fig. 2).

By fixing the midpoints to +227 and +57 mV, the data were analysed so that the intensity, maximal wavelength and bandwidth could be varied to give the best fit for each component. The results (column 3 of Table 1) favour a model with two redox components making three spectral contributions. The +58 mV component has a wavelength maximum at 557 nm and accounts for almost half of the total intensity. Subtracting this component yields a single redox component $E_{m,7}$ +227 mV with peaks at 556 and 564.8 nm, as clearly seen in Figs. 2(*d*) and 3.

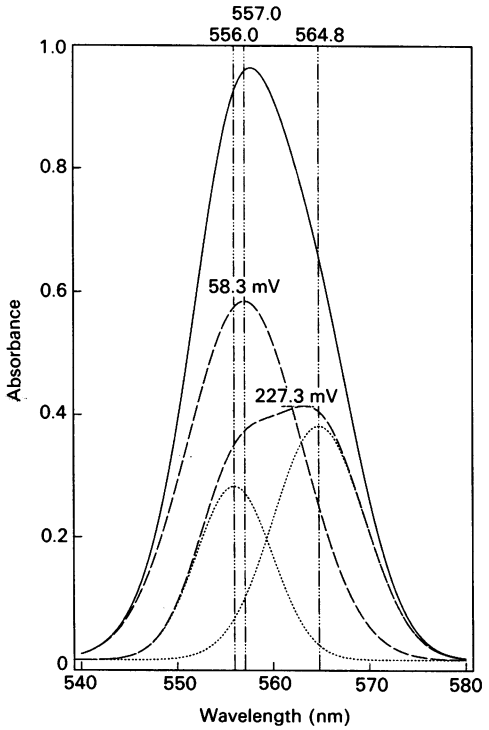

Fig. 3. Spectral components resolved from redox analysis, 540 to 580 nm

——, total absorption of fully reduced minus fully oxidized sample; – – – –, two redox components with midpoints of +58 mV (peak at 557 nm) and +227 mV; ·····, two individual absorptions which comprise the +227 mV component (peaks at 556 and 565 nm).

Potentiometric analysis of the Soret region

The Soret region of the visible spectrum of RG145 membranes could be observed in oxidative potentiometric titrations (broad trough at 426.5–427 nm with the fully reduced sample as reference) using ammonium persulphate as oxidant. The interference from change in absorbance of the redox dyes over the potential range of the experiment was less than 4%, as determined in an experiment where the cuvette contained only buffer and dyes.

Table 2. Analysis of potentiometric titrations of the Soret region

The best-fitting parameters for a four-component fit determined from analysis of area under absorbance peaks (column 1) and the redox surface by fitting each wavelength interval (column 2). Sum of squares values of statistical fit are included.

Column 1 (areas)		Column 2 (redox surface)			
$E_{m,7}$ (mV)	Amount	$E_{m,7}$ (mV)	Amount	$\lambda_{max.}$ (nm)	Bandwidth (nm)
−97	0.22	−91	0.18	428.1	26.4
55	0.48	58	0.46	425.7	16.8
211	0.22	214	0.24	429.7	18.4
408	0.14	409	0.19	426.5	12.2
Sum of squares = 0.009		Sum of squares = 0.142			

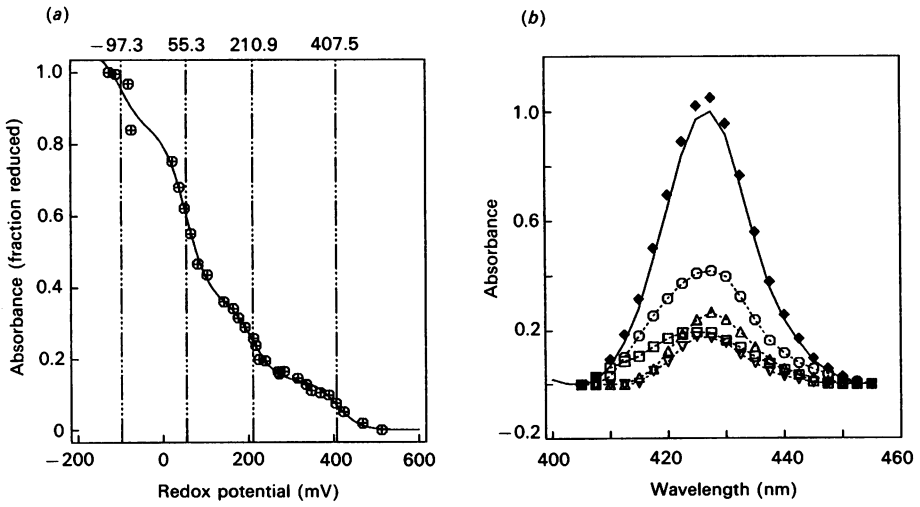

Fig. 4. A four-component fit to data based on areas under curves (400 to 455 nm)

(*a*) Best-fitting Nernst curve for a four-component fit (100% reduced = 0.75 absorbance unit). (*b*) Individual redox analysis at predicted midpoints. □, −97 mV component; ○, +55.3 mV component; △, +210.9 mV component; ▽, +407.5 mV component. ◆ symbols are experimental data; the continuous line is the predicted sum of the four components.

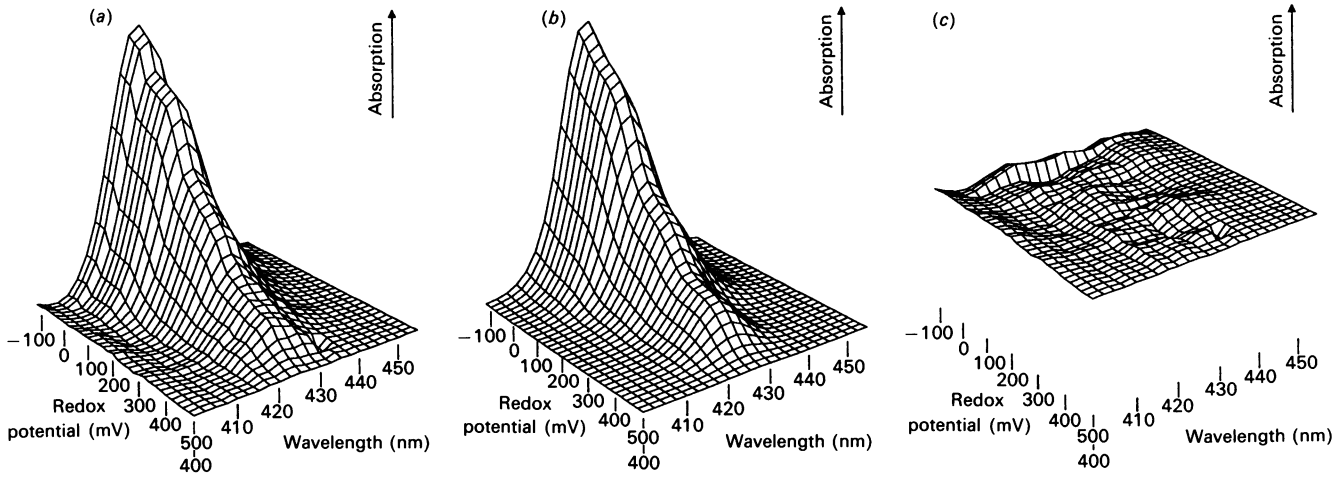

Fig. 5. Four-component fit based on redox surface analysis (400 to 455 nm)

(*a*) Actual data plotted on a regular grid (10 mV and 2.5 nm steps). (*b*) Predicted surface based on four redox components. (*c*) Difference between actual and predicted data.

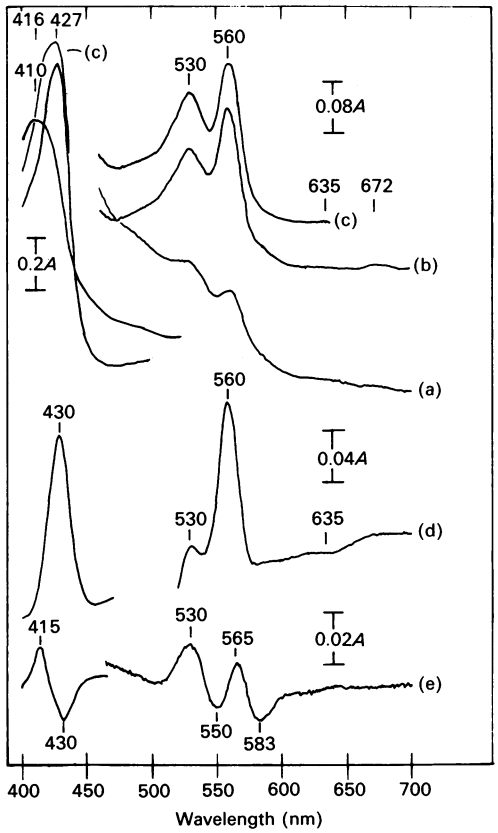

Fig. 6. Absolute and difference spectra of *E. coli* membranes at 25 °C

Traces (a)–(c) are absolute spectra of the ammonium persulphate-oxidized (a), sodium dithionite-reduced (b) and CO+reduced (c) samples. Trace (d) is the fully reduced minus fully oxidized spectrum, i.e. (b) minus (a). Trace (e) is the CO+reduced minus reduced spectrum, i.e. (c) minus (b). For the reduced+CO sample, a dithionite-reduced sample was bubbled with a steady stream of CO for 4 min. A spectrum of a 6% (w/v) suspension of dehydrated low-fat milk dissolved in 10 mM-Tes/2.5 mM-EDTA, pH 7.0, was used as subtracted baseline for 'absolute' spectra. Membranes from strain RG145 were suspended in 150 mM-Tes/3 mM-EDTA, pH 7.0, at a concentration of 10 mg/ml. Spectra were recorded in cuvettes with 1 cm pathlength and a reference wavelength of 575 nm. Scan speed = 2.9 nm/s.

From the area under the titration curve, the data clearly show three redox components titrating with midpoints $E_{m,7.0}$ of +55 mV (48%), +211 mV (22%) and +408 mV (14%) (Fig. 4*a* and Table 2, column 1). The highest-potential, but minor, component was also seen in reductive titrations; an average of +405 mV was calculated from four redox titrations, with a range from +367 to +441 mV. There is some evidence for a fourth component with a midpoint at −97 mV (22%). The wavelength maxima for those components varied from 426 to 430 nm (Fig. 4*b*). Fig. 5 shows the closeness of the fit to a four-component model.

By analysing the entire redox surface, midpoints and intensities similar to those obtained by analysis of the area were obtained (Fig. 5 and Table 2, column 2). The major component with $E_{m,7}$ of +55 to +58 mV, which accounts for over 40% of the Soret maxima at 426 nm, probably corresponds to the component titrating around +58 mV in the α region (see Table 1, column 3). The other components account for roughly 20% of the Soret intensity each. The $E_{m,7}$ = +214 mV feature, which absorbs maximally at 430 nm, probably corresponds to the broad α peak that titrates with a midpoint of +227 mV. The highest-potential component ($E_{m,7}$ = +408 mV, 427 nm) was not observed in the 560 nm region.

Identification of a high-spin component by absolute spectra

A high-spin e.p.r. signal at $g = 6.0$ has been characterized in the purified oxidase (Hata *et al.*, 1985). However, corresponding optical signals (see Wood, 1984) attributable to a high-spin component of the cytochrome *bo* complex have not been described. Absolute spectra (at room temperature) (Fig. 6) of ammonium persulphate-oxidized RG145 membranes show a broad absorbance near 630 nm and continuous absorption from 460 to 530 nm (trace a) indicative of a high-spin haem. Its γ band has a peak at 410 nm. The spectrum of the dithionite-reduced sample shows major peaks at 427 nm, 530 nm and 560 nm, and a minor peak at 672 nm (trace b); in the CO+reduced spectrum (trace c), a shoulder at 418 nm appears and small shifts in the α/β region become apparent in the CO difference spectra (trace e). The CO+reduced minus reduced spectrum shows characteristic peaks at 415, 530 and 565 nm, and troughs at 430 nm, 550 nm and 583 nm. The γ/α ratio in this spectrum, as defined by Wood (1984), is about 11. The presumptive high-spin component is also

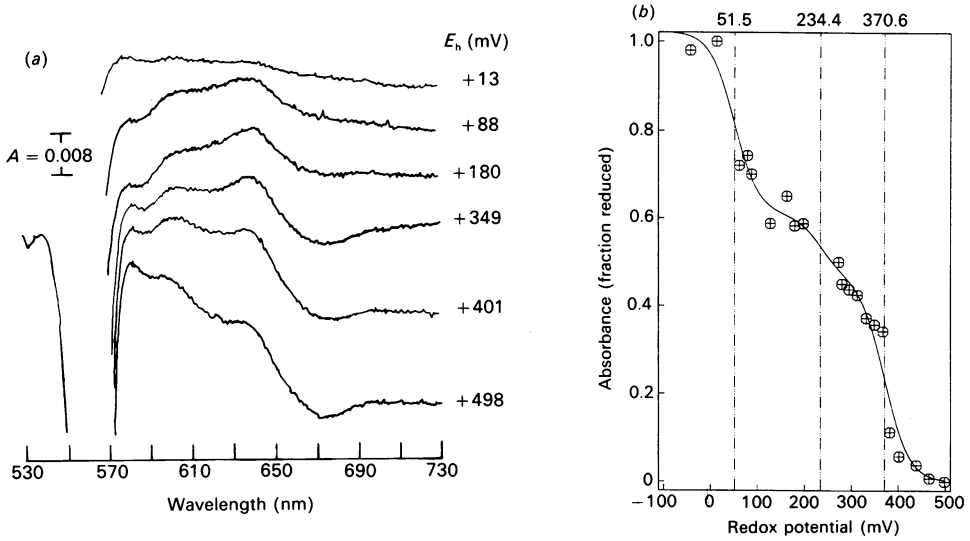

Fig. 7. Potentiometric analysis of *E. coli* membranes by difference spectroscopy (530 nm to 730 nm) at 25 °C

(*a*) Difference spectra of samples poised during an oxidative titration with ammonium persulphate as oxidant. A reduced sample poised at −110 mV was used as the subtracted baseline. Scan speed = 1.4 nm/s. (*b*) Plot of redox potential versus percentage of maximal absorbance at 635 nm minus 672 nm (100% reduced = 0.019 absorbance unit). The line represents the best-fit analysis (sum of squares = 0.031) for three components with midpoint potentials ($E_{m,7}$) of +52 mV, +234 mV and +371 mV. Membranes from strain RG145 were suspended in 150 mM-Tes/3 mM-EDTA, pH 7.0, at a concentration of 15 mg/ml. The reference wavelength was 575 nm.

visible in the fully reduced minus fully oxidized spectrum (trace d) as a broad trough from the α-peak to beyond 635 nm. The positions of the Soret peaks in the absolute spectra demonstrate that the samples were fully reduced or oxidized.

High-spin proteins containing protohaem IX generally have absorbance peaks in CO difference spectra around 538 nm and 579 nm, as for deoxymyoglobin (see Wood, 1984). In contrast, we observed peaks at 530 nm and 565 nm in CO difference spectra of *E. coli* RG145 membranes. In fact, these peak positions are nearer to those seen in cytochromes *c'*, high-spin *c*-type haems (Bartsch, 1963). Although *E. coli* has been found to synthesize a cytochrome *c*-552 which may be involved in sulphite reduction (see Poole & Ingledew, 1987), we scanned pyridine haemochrome spectra of the extract and pellet fractions from acid/acetone-treated membranes to rule out the possibility of a high-spin cytochrome *c* being present in the membranes. Haems *c* are not extracted by acid/acetone and are found in the residue with a peak at 551 nm as the dithionite-reduced pyridine haemochrome. All of the cytochrome haem absorbance from membranes was found in the acid/acetone extract with a peak at 555 nm in reduced minus oxidized pyridine haemochrome spectra, confirming that no cytochrome *c* was present. The observed peak at 555 nm for the extract is close to the myoglobin pyridine haemochrome at 557 nm (reduced minus oxidized), whereas the β band at 522.5 nm is atypical of a *b*-type haem (β band of myoglobin at 526 nm) and is closer to values observed for *c*-type haems.

In an oxidative titration (Fig. 7*a*), performed by adding ammonium persulphate to a dithionite-reduced sample, we monitored the absorbance change at 635 nm minus 672 nm. Three $n = 1$ components were found with midpoints ($E_{m,7}$) of +52 mV (41%), +234 mV (14%) and +371 mV (47%) (Fig. 7*b*). These presumably correspond to components observed at these potentials in the Soret and α regions. The change in the $A_{560-580}$ band in this titration gave the expected E_m values (not shown), as determined previously at this wavelength (see Table 2). The identity of components contributing to these changes is unknown and the data could be analysed by plotting other wavelength pairs.

DISCUSSION

Assignment of redox components

Area and surface analyses of redox titrations from *E. coli* strain RG145 suggest two redox components in the α region: a cytochrome *b* with a peak at 557 nm ($E_{m,6.85} = +57$–58 mV) accounting for about one-half of the total absorbance and a redox component with a broad or split peak absorbing at 556–564 nm, with $E_{m,6.85} = +227$ mV. Redox components with midpoints similar to these were also observed in the Soret region. Additionally, at about 426 nm and 635 nm a component with a midpoint potential around +400 mV was detected. Although the membranes of the amplified strain RG145 contain a higher concentration of the cytochrome *bo* complex than do membranes of wild-type strains, there may still be some contribution to absorbance at 560 nm from other *b*-type cytochromes. The succinate dehydrogenase-associated cytochrome *b*-556, for example, has a midpoint ($E_{m,7}$) of −45 mV in membranes (Kita *et al.*, 1989). The lowest-potential component that we sometimes see ($E_{m,7}$ −50 to −100 mV) may be equivalent to this.

The midpoint values determined in this report are similar to those described by Reid & Ingledew (1979) and van Wielink *et al.* (1982) for membranes of aerobically grown cells. We did not observe a component titrating with $E_{m,7}$ of around +150 mV, as found with the purified enzyme (Kita *et al.*, 1984) or in cytochrome *d*-deficient membranes (Lorence *et al.*, 1984).

The published absorbance coefficients for total cytochrome *b* ($\epsilon_{560-580}$ of 18.7 $mM^{-1} \cdot cm^{-1}$ from reduced minus oxidized spectra) and cytochrome *o* ($\epsilon_{415-430}$ of 145 $mM^{-1} \cdot cm^{-1}$ from CO difference spectra) (Kita *et al.*, 1984) appear incompatible with the present data. From an average of seven membrane preparations from strain RG145, about 70% of the total *b*-type cytochrome appears to be attributable to cytochrome *o*. The redox component with a peak at 557 nm, however, accounts for about half of the total absorbance in fully reduced minus oxidized spectra of the α region, suggesting that the absorption coefficient for cytochrome *o* may be slightly underestimated.

There are two explanations of the α-band data. The first invokes anti-co-operative interaction between the haems (Salerno

et al., 1989, 1990). In the higher-potential transition (+227 mV) part of the cytochrome *o* and part of the other *b*-type cytochrome may be reduced, giving a split α-band (Fig. 3). Approx. 40% of the *b*-type cytochrome and 60% of cytochrome *o* are reduced in the high-potential transition. However, a spectrum recorded at +58 mV shows only a single peak at 557 nm (Fig. 3). This could be explained by a shift to shorter wavelengths in the α-band of cytochrome *o* when the other *b*-type cytochrome is reduced, such that the 557 nm 'peak' is composed of two contributions. Thus at 77 K the maximum for cytochrome *o* is around 564 nm when cytochrome *b* is oxidized, but at 561 nm when cytochrome *b* is reduced. An alternative explanation of the data would involve both components of the split or broad peak 556–565 nm being attributable to the cytochrome *o* component.

The high-potential changes seen in the Soret region may be effects of the reduction of the Cu^{2+} centre on the spectrum of the binuclear Cu-*o* centre (~ +400 mV). A coupling between cytochrome a_3^{3+} and Cu_B of the mitochondrial oxidase, resulting in a peak at 655 nm, has been hypothesized (Beinert *et al.*, 1976; Karlson & Andréasson, 1981).

Comparison of optical and e.p.r. analysis

Similar potentiometric analyses conducted using e.p.r. measurements at 15 K gave indirect evidence of a copper centre titrating at approx. +370 mV, and the cytochrome *o* and *b* both titrating at +280 mV and +180 mV. Qualitatively the pattern of the data is the same, although the apparent midpoint-potential values differ somewhat. We might explain this discrepancy by an effect of temperature. Although in both cases the redox titrations are performed at room temperature, in the e.p.r. experiments the samples are frozen and monitored at approx. 15 K. Differences between the optically and e.p.r.-determined values are also a feature of mammalian cytochrome aa_3 (see Wikström *et al.*, 1981). Electron equilibration between centres occurs rapidly even at 5 K (Leigh *et al.*, 1974). We find that when the same e.p.r. samples are measured optically at 77 K, the midpoint values obtained for components at 555 nm and 564 nm are close to those from the e.p.r. data (B. Bolgiano, J. C. Salerno & W. J. Ingledew, unpublished work).

Studies of bacterial cytochrome oxidases have continued to yield interesting results not only by providing a simpler model for studying the complex reactions of metal centres in common with the mammalian aa_3-type oxidases, but also by revealing intriguing information on the evolution of oxygen-utilizing enzymes in rather primitive organisms. The apparent complexity of haem–haem interactions in the cytochrome *o*-type oxidase of *E. coli* is one such example.

We are grateful to Robert Gennis for providing the *E. coli* strains used in this work, to John Salerno and Paul Wood for intriguing discussions and to Martyn Sharpe for preparation of cytoplasmic membranes from strain GO103. This work was supported by a grant from the Science and Engineering Research Council to R. K. P. and W. J. I. R. K. P. thanks the Royal Society and Smith–Kline Foundation for equipment grants.

REFERENCES

Au, D. C.-T. & Gennis, R. B. (1987) J. Bacteriol. **169**, 3237–3242
Bartsch, R. G. (1963) in Bacterial Photosynthesis (Gest, H., San Pietro, A. & Vernon, L. P., eds.), pp. 475–494, Antioch Press, Yellow Springs, OH
Beinert, H., Hansen, R. E. & Hartzell, C. R. (1976) Biochim. Biophys. Acta **423**, 339–355
Castor, L. N. & Chance, B. (1959) J. Biol. Chem. **234**, 1587–1592
Chance, B., Smith, L. & Castor, L. (1953) Biochim. Biophys. Acta **12**, 289–298
Chance, B., Saronio, C., Leigh, J. S., Jr., Ingledew, W. J. & King, T. E. (1978) Biochem. J. **171**, 787–798
Chepuri, V., Lemieux, L., Au, D. C.-T. & Gennis, R. B. (1990) J. Biol. Chem. **265**, 11185–11192
Dutton, P. L. (1978) Methods Enzymol. **54**, 411–435
Erecinska, M. & Chance, B. (1972) Arch. Biochem. Biophys. **151**, 304–315
Fuhrhop, J.-H. & Smith, K. M. (1975) in Porphyrins and Metalloporphyrins (Smith, K. M., ed.), pp. 804–807, Elsevier/North-Holland, Oxford and New York
Georgiou, C. D., Dueweke, T. J. & Gennis, R. B. (1988) J. Bacteriol. **170**, 961–966
Gibson, F., Cox, G. B., Downie, J. A. & Radik, J. (1977) Biochem. J. **164**, 193–198
Gill, P. E. & Murray, W. (1972) J. Inst. Math. Its Appl. **9**, 91–108
Hata, A., Kirino, Y., Matsuura, K., Itoh, S., Hiyama, T., Konishi, K., Kita, K. & Anraku, Y. (1985) Biochim. Biophys. Acta **810**, 62–72
Holm, L.,Saraste, M. & Wikstrom, M. (1987) EMBO J. **6**, 2819–2823
Karlson, B. & Andréasson, L.-E. (1981) Biochim. Biophys. Acta **635**, 73–80
Kita, K., Konishi, K. & Anraku, Y. (1984) J. Biol. Chem. **259**, 3368–3374
Kita, K., Vibat, C. R. T., Meinhardt, S., Guest, J. R. & Gennis, R. B. (1989) J. Biol. Chem. **264**, 2672–2677
Kranz, R. G. & Gennis, R. B. (1985) J. Bacteriol. **161**, 709–713
Leigh, J. S., Jr., Wilson, D. F., Owen, C. S. & King, T. E. (1974) Arch. Biochem. Biophys. **160**, 476–486
Lorence, R. M., Green, G. N. & Gennis, R. B. (1984) J. Bacteriol. **157**, 115–121
Markwell, M. A. K., Haas, S. M., Bieber, L. L. & Tolbert, N. E. (1978) Anal. Biochem. **87**, 206–210
Matsushita, K., Patel, L. & Kabak, H. R. (1984) Biochemistry **23**, 4703–4714
Miller, J. (1972) Experiments in Molecular Genetics, p. 440, Cold Spring Harbor Laboratory, Cold Spring Harbor
Müller, M., Schlapfer, B. & Azzi, A. (1988) Proc. Natl. Acad. Sci. U.S.A. **85**, 6647–6651
Pirt, S. J. (1967) J. Gen. Microbiol. **47**, 181–197
Poole, R. K. (1988) in Bacterial Energy Transduction (Anthony, C., ed.), pp. 231–291, Academic Press, London and New York
Poole, R. K. & Chance, B. (1981) J. Gen. Microbiol. **126**, 277–287
Poole, R. K. & Ingledew, W. J. (1987) in *Escherichia coli* and *Salmonella typhimurium* Cellular and Molecular Biology (Neidhardt, F. C., Ingraham, J. L., Low, K. B., Magasanik, B., Schaechter, M. & Umbarger, H. E., eds), pp. 170–200, American Society for Microbiology, Washington
Poole, R. K., Waring, A. J. & Chance, B. (1979) Biochem. J. **184**, 379–389
Poole, R. K., Williams, H. D., Downie, J. A. & Gibson, F. (1989) J. Gen. Microbiol. **135**, 1865–1874
Reid, G. A. & Ingledew, W. J. (1979) Biochem J. **182**, 465–472
Rieske, J. S. (1967) Methods Enzymol. **10**, 488–492
Rothery, R. A., Houston, A. M. & Ingledew, W. J. (1987) J. Gen. Microbiol. **113**, 3247–3255
Salerno, J. C., Bolgiano, B. & Ingledew, W. J. (1989) FEBS Lett. **247**, 101–105
Salerno, J. C., Bolgiano, B., Poole, R. K., Gennis, R. B. & Ingledew, W. J. (1990) J. Biol. Chem. **265**, 4364–4368
van Wielink, J. F., Oltman, L. F., Leeuwerik, F. J., DeHollander, J. A. & Stouthamer, A. H. (1982) Biochim. Biophys. Acta **681**, 177–190
Wikström, M., Krab, K. & Saraste, M. (1981) Cytochrome Oxidase: A Synthesis, Academic Press, New York and London
Williams, H. D. & Poole, R. K. (1987) J. Gen. Microbiol. **133**, 2461–2472
Wilson, D. F. & Leigh, J. S., Jr. (1972) Arch. Biochem. Biophys. **150**, 154–163
Wood, P. M. (1984) Biochim. Biophys. Acta. **768**, 293–317

Received 27 April 1990/3 October 1990; accepted 24 October 1990